Parasitol Res (2003) 91: 151–165
DOI 10.1007/s00436-003-0941-3

ORIGINAL PAPER

Elizabeth G. Moodie · Leo F. Le Jambre
Margaret E. Katz

Thelohania parastaci sp. nov. (Microspora: Thelohaniidae), a parasite of the Australian freshwater crayfish, *Cherax destructor* (Decapoda: Parastacidae)

Received: 27 May 2003 / Accepted: 11 June 2003 / Published online: 16 August 2003

Abstract *Thelohania parastaci* sp. nov. infects the Australian freshwater crayfish, *Cherax destructor*. Data on morphology, developmental patterns and sequences from the small subunit (SSU) and internal transcribed spacer (ITS) regions of the ribosomal DNA (rDNA) of *T. parastaci* sp. nov. are described. The ultrastructural features of different life cycle stages are very similar to those of the European crayfish parasite *Thelohania contejeani*. *T. parastaci* sp. nov. exhibits simultaneous dimorphic sporogony in muscle tissue. Meronts, sporonts and spores are found in muscle tissue, within haemocytes in the hepatopancreas, and in the intestinal wall of infected crayfish. *T. parastaci* sp. nov. shows 92% sequence identity with *T. contejeani* and only 67% sequence identity with the fire ant pathogen *T. solenopsae*, when SSU rDNA sequences are compared. Analysis of SSU rDNA and ITS sequences of *T. parastaci* sp. nov. from crayfish from Victoria, Western Australia, and New South Wales indicate that the parasite has a wide geographical distribution in Australia.

Introduction

The microsporidian genus *Thelohania* Henneguy, 1892 (Henneguy and Thelohan 1892) includes a number of species that are significant intracellular parasites of decapod crustaceans such as crabs, prawns and freshwater crayfish (Alderman and Polglase 1988; Sindermann 1990). At least six species are found in crustacean hosts other than crayfish (Knell et al. 1977) and over 60 species have been described from insect hosts (Becnel and Andreadis 1999). Despite much research effort, no complete life cycle for any species of *Thelohania* has yet been described.

In crustaceans, muscle tissue is targeted by the parasite and deterioration in muscle function eventually results in death of the host (Cossins 1973). The type species for the genus is *T. giardi* Henneguy, 1892, (Henneguy and Thelohan 1892), a parasite of the European marine shrimp *Crangon crangon* (Linnaeus, 1758), synonymous with *Crangon vulgaris* Fabricius, 1798. Unfortunately, no data on ultrastructure or molecular characteristics are available for the type species.

Two *Thelohania* species which parasitize freshwater crayfish have been described; *T. contejeani* Henneguy, 1892, a parasite of the European crayfish *Astacus fluviatilis* L. (Henneguy and Thelohan 1892) and *T. cambari* Sprague, 1950 (Sprague 1950), a parasite of the North American crayfish *Cambarus bartonii* (Fabricius 1798) (Sprague 1950). Lom et al. (2001) reviewed what is known of the ultrastructure, life cycle features and taxonomic affinities of *T. contejeani*. They were the first authors to describe its dimorphic pattern of sporogony and provide molecular data, i.e. the small subunit ribosomal DNA (SSU rDNA) sequence, for a *Thelohania* parasite of a crustacean host.

France and Graham (1985) identified a microsporidian parasite of the North American crayfish *Orconectes virilis* (Hagen, 1870) as *T. contejeani*. Quilter (1976) also referred to a microsporidian parasite of the New Zealand crayfish, *Paranephrops zealandicus* White, 1842 as *T. contejeani*. Data on fine ultrastucture or molecular characteristics were not collected in either of these studies.

Prior to this study, all reports of *Thelohania* in Australian freshwater crayfish have been of undescribed species infecting the yabby *Cherax destructor* (Clark, 1936), redclaw *Cherax quadricarinatus* (von Martens, 1868), gilgy *Cherax quinquecarinatus* (Gray, 1845), and

E. G. Moodie (✉)
Zoology, School of Biological, Biomedical and Molecular Sciences, University of New England, NSW 2351 Armidale, Australia
E-mail: emoodie@pobox.une.edu.au

L. F. Le Jambre
CSIRO Livestock Industries, Locked Bag 1, NSW 2350 Armidale, Australia

M. E. Katz
Molecular and Cellular Biology, School of Biological, Biomedical and Molecular Sciences, University of New England, NSW 2351 Armidale, Australia

marron *Cherax tenuimanus* (Smith, 1912), as outlined in a review by O'Donoghue and Adlard (2000). In Australia, reported prevalences of infection of *C. destructor* by *Thelohania*, as determined by microscopic examination for spores, have varied from < 1% (Carstairs 1979) to 38% (O'Donoghue et al. 1990) in yabby populations from rivers, swamps and lakes in New South Wales, Victoria and South Australia. Comprehensive surveys of cultured populations of *C. destructor* have not been carried out. However, in a recent survey of *Cherax destructor albidus* (Austin 1996) cultured in farm dams in the southwestern region of Western Australia, yabbies from 48 of 157 sample sites (31%) were found to be infected with *Thelohania* (Jones and Lawrence 2001).

The objectives of this study were to describe a new Australian species of *Thelohania*, *T. parastaci* sp. nov., a parasite of cultured and wild stocks of the yabby *C. destructor,* and to compare this new species with other *Thelohania* species using both ultrastructural and molecular data.

Materials and methods

Sources of infected hosts

Adult yabbies of both sexes belonging to three subspecies; *C. destructor albidus* (Austin 1996), *C. d. rotundus* (Austin 1996), and *C. d. destructor* (Austin 1996) were sampled. The sampling locations and host codes are described in Table 1. All yabbies were heavily parasitized with extensive whitening of the abdominal flexor muscles, usually visible through the ventral carapace, due to the presence of microsporidian spores.

Light microscopy

Microsporidian infection was initially confirmed by examination of fresh squashes of 0.25–0.5 mm^3 of abdominal muscle or anterior pleopod muscle at high power under a light microscope. Impression smears of infected abdominal muscle were stained with 10% Giemsa. Semi-thin sections of tissue processed for electron microscopy (see below) were stained with 1% toluidine blue. Samples of fresh muscle tissue were stored frozen and later thawed for spores to be photographed and measured (Undeen 1997). Measurements were made using Photoshop 5.5 (Adobe; San Jose, USA) software.

Transmission electron microscopy

Samples of fresh yabby tissue, including abdominal muscle, hepatopancreas, intestine and ovary were fixed for 6 h or overnight at 4°C in either 2.5% gluteraldehyde in 0.1 M cacodylate buffer (pH 7.4), or in a mixture of 2% gluteraldehyde, 2% paraformaldehyde and 0.5% dimethyl sulphoxide in 0.1 M cacodylate buffer (pH 7.4) containing 8 mM $CaCl_2$ (J. Mathews, personal communication). Overnight fixation in the latter fixative produced the best results. Fixed tissues were washed 5 times in fresh 0.1 M cacodylate buffer and postfixed for 1–2 h in 1% osmium tetroxide. A 2% uranyl acetate bloc stain was performed at the second stage of dehydration through a graded acetone series, and the tissue embedded in Spurr's resin. Ultra-thin sections were post stained in uranyl acetate and lead citrate prior to examination with a Jeol JEM 1200 EX electron microscope, operated at 60 kV.

DNA extraction

Spores from approximately 0.5 g of heavily infected abdominal muscle were purified by digestion in 10 ml of 2% pepsin (w/v) in 0.5% HCl (v/v) for 1 h at 37°C (Langdon 1991), pelleted by centrifugation at 1,800 *g* for 10 min and washed in sterile distilled water 4 times. The spore pellet was suspended in 50 µl extraction buffer (100 mM NaCl, 10 mM TRIS-HCl, pH 8.0, 25 mM EDTA, 0.5% SDS), frozen and thawed 3 times, and then ground for 30 s in a 1.5-ml microfuge tube with a micropestle attached to a hand-held electric drill. Extraction buffer (450 ml) was added and the suspension incubated overnight at 37°C with proteinase K (200 µg per ml final concentration). The proteinase K was inactivated by heating the solution for 5 min at 95°C. After cooling to room temperature, the extract was incubated with RNase (100 µg per ml final concentration) for 30 min at 37°C.

Genomic DNA in the digestion solution was purified by extraction in phenol/chloroform/isoamyl alcohol (25:24:1), followed by extraction in chloroform/isoamyl alcohol (24:1). The purified DNA was precipitated with ethanol, dissolved in 100 µl TE buffer (10 mM TRIS-HCl, pH 8.0, 1 mM EDTA) at 65°C for 1 h, and stored at −20°C. DNA concentration was determined spectrophotometrically by measuring absorbance at wavelengths of 260 nm and 280 nm.

Table 1 Sources of microsporidian DNA from yabbies. *SSU* Small subunit, *ITS* internal transcribed spacer, *NSW* New South Wales

Yabby subspecies	Location (latitude, longitude)	Microsporidian species	Code for SSU rDNA sequence	Code for ITS sequence
Cherax destructor albidus	Dam in West Wimmera region, Victoria (37°4′S, 141°19′E)	*Thelohania parastaci* sp. nov.	WW1, WW2	WW1, WW2, WW3, WW5
	Dams from SW Western Australia (31°56′S, 115°58′E)	*T. parastaci* sp. nov.	WA1, WA2, WA5	WA1, WA2, WA4, WA5
Cherax destructor destructor	Tumut River catchment (35°20′S, 148°16′E)	*T. parastaci* sp. nov.	TUM	not sequenced
Cherax destructor rotundus	Creek in Karuah River catchment, NSW (32°45′S, 151°44′E)	*T. parastaci* sp. nov.	R1, R2, R7, E236	R1, R2, R4, R7, E236
C. d. destructor	Tea Tree Creek, Armidale, NSW (30°30′S, 151°40′E)	*Thelohania montirivulorum* (Moodie et al. 2003)	Tx3, SKH	Tx3

Table 2 Primers used to amplify and sequence *T. parastaci* sp. nov. For abbreviations, see Table 1

Primer	5′ → 3′ sequence	Melting temperature (°C)
SSU rDNA		
Forward		
18f	CACCAGGTTGATTCTGCC	56.0
w302f	GCGAAACTTACCCAATGCTA	61.5
T423f	GGCTTAATTTGACTCAACGC	58.0
Reverse		
1492r	GGTTACCTTGTTACGACTT	54.0
T423r	GCGTTGAGTCAAATTAAGCC	55.3
V420r	AACAAGTATTACCGCGGCTG	60.0
ITS rDNA		
Forward		
w1243f	GCCCGTCGTTATCTCAGATG	64.5
Reverse		
BBAr	TCCNRGTTRGTTTCTTTTCCT	61.0

PCR protocol

To amplify SSU rDNA, the universal primers 18f and 1492r (Weiss and Vossbrinck 1998) were used (Table 2). Each 50 µl of PCR reaction mix contained 5 µl of 10× reaction buffer without $MgCl_2$ (Promega, Madison, Wis.), 1.5 mM $MgCl_2$, 0.2 mM dNTPS, 25 pmol of each primer, 1.25 units of Taq DNA polymerase (Promega) and 120 ng of template DNA. PCR amplifications were performed as follows on a Mastercycler gradient thermocycler (Eppendorf, Hamburg): after an initial denaturation for 2 min at 94°C, samples were subjected to 35 cycles of amplification (denaturation at 94°C for 1 min, primer annealing at 48°C for 1 min, and extension at 68°C for 2 min), followed by a 10 min final extension at 68°C. The relatively low extension temperature was used to enhance amplification of DNA with a low GC content (R. Gasser, personal communication). A fragment of 1,337 bp was amplified.

The internal transcribed spacer region (ITS), including the 3′ end of the SSU and the 5′ end of the large subunit rDNA genes, was amplified with the primers w1243f and BBAr (Table 2). Fifty microlitre reactions were prepared in the same way as for amplification of the SSU rDNA, and PCR was performed under the same conditions, except that an annealing temperature of 50°C was used. A fragment of approximately 350 bp was amplified.

Sequencing

Amplified PCR products were purified with the Wizard PCR Preps purification system (Promega) and sequenced with the universal primers 18f and 1492r, and a series of internal primers described in Table 2. Where more than one band was amplified, the relevant band was cut out of a 0.8% agarose gel, frozen for 10 min, thawed, eluted by high speed centrifugation in a Ultrafree-MC 0.45 µm centrifugal filter tube (Millipore, Bedford, Mass.), and purified using Wizard PCR Preps (Promega). Sequencing was performed by Newcastle DNA (Newcastle, Australia) using Big Dye kit dye terminator chemistry and an automated ABI PRISM 377 DNA sequencer (Applied Biosystems, Richmond, Va.).

A BLASTN search in Genbank (Altschul et al. 1997) was used to compare the sequences obtained to those available on the Genbank database. Sequence similarities were estimated with PAUP* version 4.0b9 for Windows (Swofford 2000). GC contents of SSU rDNA gene sequences were calculated using SeqaidII Version 3.8 (Rhoads and Roufa 1990).

Results

T. parastaci sp. nov. was found in adult yabbies of both sexes from farm dam populations of the yabby subspecies *C. d. albidus* in Victoria and Western Australia, a stream-dwelling population of *C. d. destructor* in southern New South Wales, and stream-dwelling populations of *C. d. rotundus* in central New South Wales. *T parastaci* sp. nov. was not found in a highland population of *C. d. destructor* from near Armidale in New South Wales where a different species was detected (Moodie et al. 2003). Type specimens of *T. parastaci* sp. nov. were submitted to the Queensland Museum (registration nos. G463715 and G463716-G463719 for hapantotypes and parahapantotypes, respectively).

Light microscope observations of fresh and stained spores

T. parastaci sp. nov. exhibited dimorphic sporogony in muscle tissue, with simultaneous production of uninucleate spores within sporophorous vesicles (SPVs) and binucleate (diplokaryotic) spores in direct contact with host cell cytoplasm. SPVs containing eight uninucleate spores were found in moderate numbers, and were most abundant in myocytes (Figs. 1, 2). Free diplokaryotic spores were very common, and in smears of infected tissue they often occurred in pairs (Fig. 3). Fresh spores were lozenge shaped with rounded ends. Unfixed free spores averaged 3.9 µm (range of 3.2–4.9 µm) in length and 2.0 µm (range of 1.5–2.7 µm) in width ($n = 80$). SPVs were generally elliptical in shape, with average maximum and minimum diameters of 8.8 µm and 7.3 µm, respectively ($n = 16$). Shrinkage occurred with fixation. Spores from different yabbies showed some variation in size. Spores from SPVs appeared to be of similar dimensions to free spores.

Heavily infected muscle cells full of spores were often found adjacent to uninfected muscle cells (Fig. 4). Very high densities of spores were found in abdominal and thoracic muscle tissue and in muscle associated with the appendages including pleopods and chelae. Lower numbers were found in heart muscle, muscle associated with the digestive tract, in haemolymph channels of gill filaments, and in haemocytes in the hepatopancreas. No spores or earlier stages were found in semithin sections of ovarian tissue. Usually there were no signs of a host inflammatory response to *T. parastaci* sp. nov., although in one heavily infected yabby (TUM), the myocyte cell membranes had ruptured and haemocytes were common.

Electron microscope findings

Groups of meronts and sporonts were interspersed with clusters of free mature spores and SPVs in muscle tissue. Mature spores were far more common than earlier stages

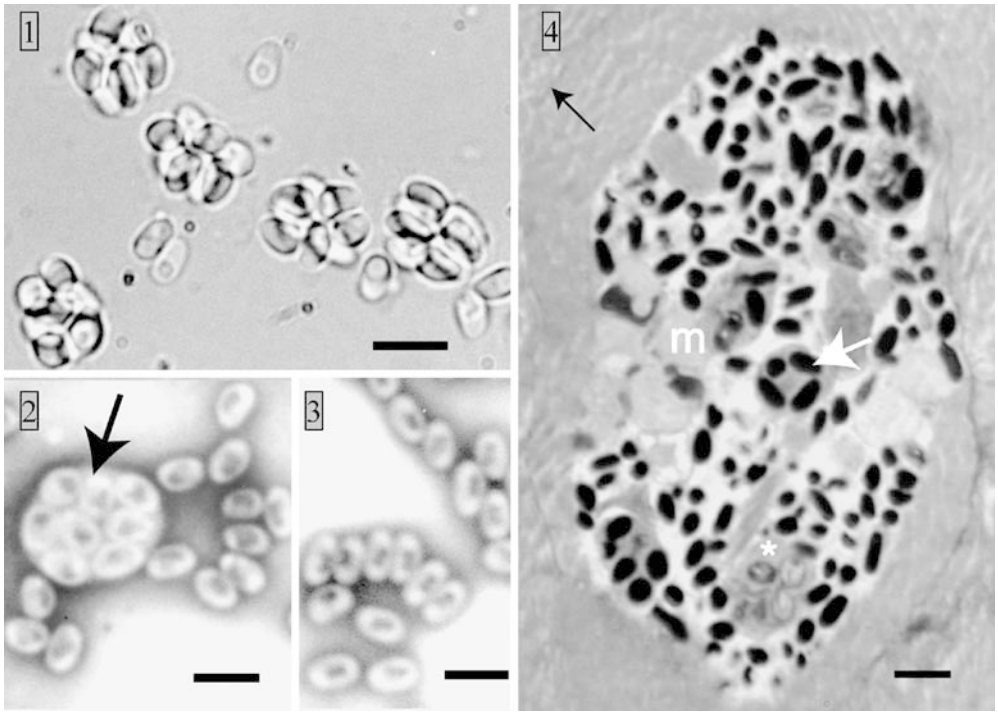

Fig. 1 Light micrograph of fresh unstained sporophorous vesicles (SPVs), each containing eight spores, and a small number of free spores. *Scale bar* 5 μm

Fig. 2 Light micrograph of a Giemsa-stained SPV (→) containing eight spores. *Scale bar* 5 μm

Fig. 3 Light micrograph of Giemsa-stained, free diplokaryotic spores. *Scale bar* 5 μm

Fig. 4 Light micrograph of a toluidine-stained section showing an infected muscle cell with intact plasmalemma (*black arrow*). In the section are meronts (*m*), sporoblasts (*) and mature spores within SPVs (*white arrow*). *Scale bar* 5 μm

in tissues from heavily infected yabbies. The meronts from which the two different spore types were derived could not be differentiated. SPVs formed around sporonts in association with thickening of the sporont wall. At this stage, the two pathways for spore development could be distinguished. Developing meronts, sporonts and mature spores were found within haemocytes in the hepatopancreas. The pattern of sporogony in haemocytes appeared similar to the production of diplokaryotic spores in muscle tissue. No SPVs were observed in these cells. The different developmental stages of *T. parastaci* sp. nov. are discussed in detail in the following sections. Host mitochondria were often seen in close proximity to the early developmental stages.

Meronts

Diplokaryotic meronts were found in abdominal muscle cells (Figs. 5, 6), within haemocytes in the hepatopancreas (Figs. 7, 8, 9, 10) and in the intestinal wall in association with muscle tissue (Fig. 11). Short tubules were visible adjacent to the outer plasmalemma of some meronts (Fig. 6). Spindle-shaped early meronts were observed in haemocytes but not in other tissues (Figs. 7, 8). Meronts in haemocytes were observed undergoing binary fission (Fig. 9). In all tissues, including haemocytes (Fig. 10), late meronts and sporonts were globular in shape. Transformation of meronts to sporonts was associated with reduction in cell diameter, thickening of the plasmalemma, increased electron density of the cytoplasm and more numerous vesicles in the cytoplasm (Figs. 11, 12).

Sporonts

Sporonts in muscle tissue appeared similar to those in haemocytes (Figs. 13, 14). Small vesicles, 80–90 nm in diameter, visible in the cytoplasm of the sporonts in Fig. 13, are suggestive of mitochondrial remnants discovered in the microsporidian *Trachipleistophora hominis* (Williams et al. 2002). One sporont was seen that differed from the others (Fig. 15). It was more elongated, contained relatively few vesicles and was rich in endoplasmic reticulum. It is possible that this sporont type is responsible for the production of diplokaryotic spores. The envelope around the diplokaryotic sporont in Fig. 15 differed in structure to the SPV developing around the sporont in Fig. 13. No tubular material was evident in the envelope of the elongated sporont. Division of binucleate sporonts by binary fission (Fig. 14) in the absence of SPV formation suggested the development of binucleate rather than uninucleate spores within haemocytes. Unfortunately, the nuclei of mature spores

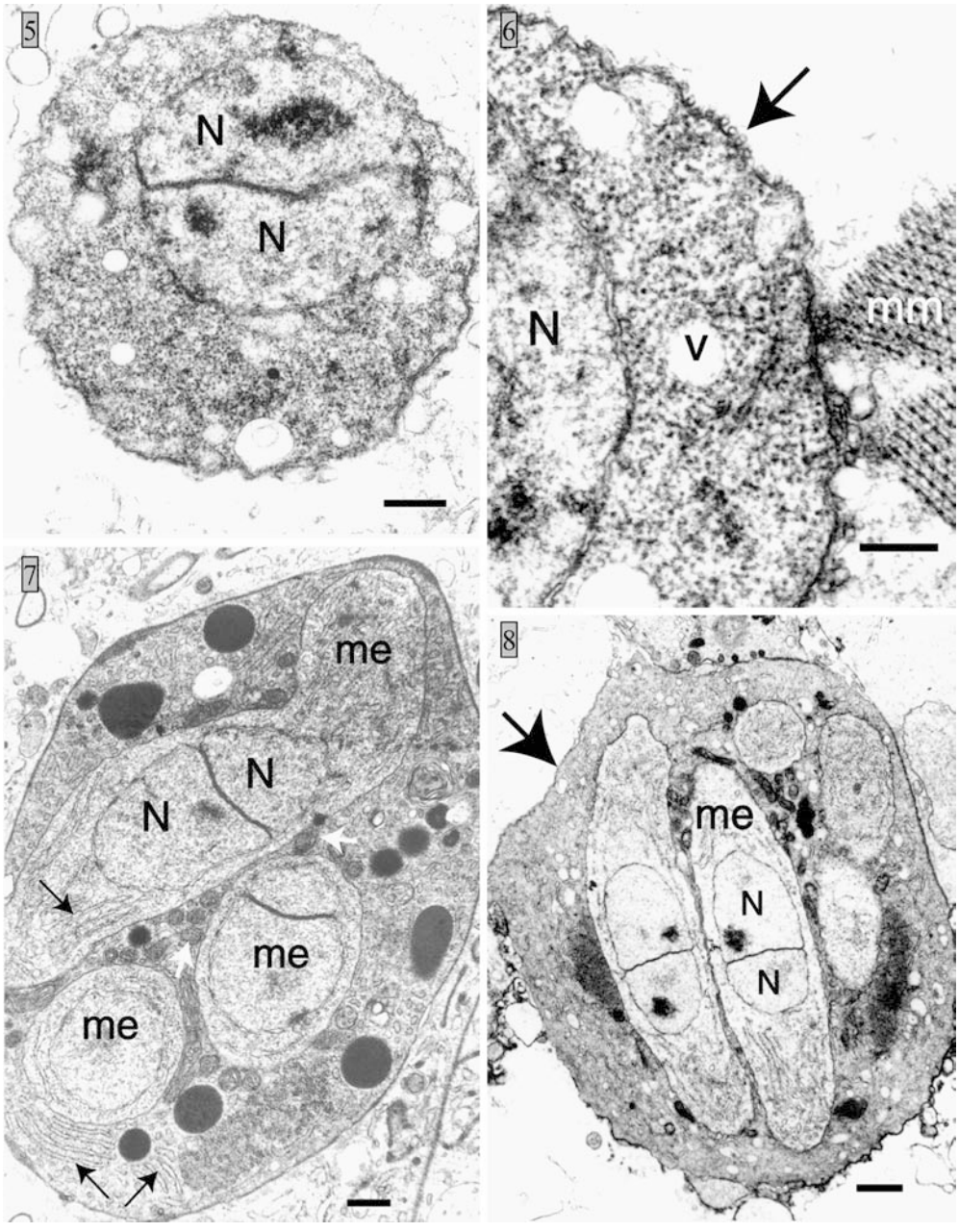

Fig. 5 Electron micrograph of binucleate meront with diplokaryotic nuclei (*n*), in muscle cell. *Scale bar* 500 nm

Fig. 6 Meront adjacent to intact muscle fibres (*mm*) in muscle cell. Small tubular structures (→) evident on outer membrane of meront. One of the meront nuclei (*N*) is visible. Meront cytoplasm is vacuolated (*v*). *Scale bar* 200 nm

Fig. 7 Haemocyte containing three meronts (*me*). Diplokaryotic nuclei (*N*) visible in elongated meront. Endoplasmic reticulum (*black arrows*) clearly visible in meronts and host cell. Host mitochondria (*white arrows*) are located close to the meronts. *Scale bar* 1 μm

Fig. 8 Spindle shaped meronts (*me*) within a crayfish haemocyte (→). The nuclei (*N*) have prominent nucleoli. *Scale bar* 1 μm

in haemocytes were not clearly seen in any sections. Binary fission of the sporont presumably preceded sporoblast development. Binary fission of sporonts within SPVs in muscle tissue was not observed.

Sporophorous vesicles

In Giemsa-stained sections, SPVs containing two, four and eight nuclei were observed. Only uninucleate spores developed within SPVs. Characteristic microtubules and fibrous macrotubules, similar to those of *T. contejeani* (Lom et al. 2001), were found in the episporontal spaces of SPVs (Figs. 16, 17). The average diameter of microtubules was 73 nm (range 50–99 nm, $n = 40$), whereas macrotubules averaged 249 nm (range 205–307 nm, $n = 40$) in diameter. Microtubules appeared to contribute to development of the spore coat. The number of free microtubules not associated with spore walls decreased as sporoblasts matured. The density of macrotubules varied between SPVs and did not seem to be clearly related to maturation events. Aggregations of granular material (dense bodies) were seen in the early stages of sporoblast development within SPVs (Fig. 18). Dense bodies were closely associated with sporoblast walls (Fig. 19) and in vesicles with more mature sporoblasts they were no longer evident (Figs. 20, 21, 22). Binucleate spores developed in pairs surrounded by fragile vesicles (Fig. 23), possibly derived from the envelope seen in Fig. 15.

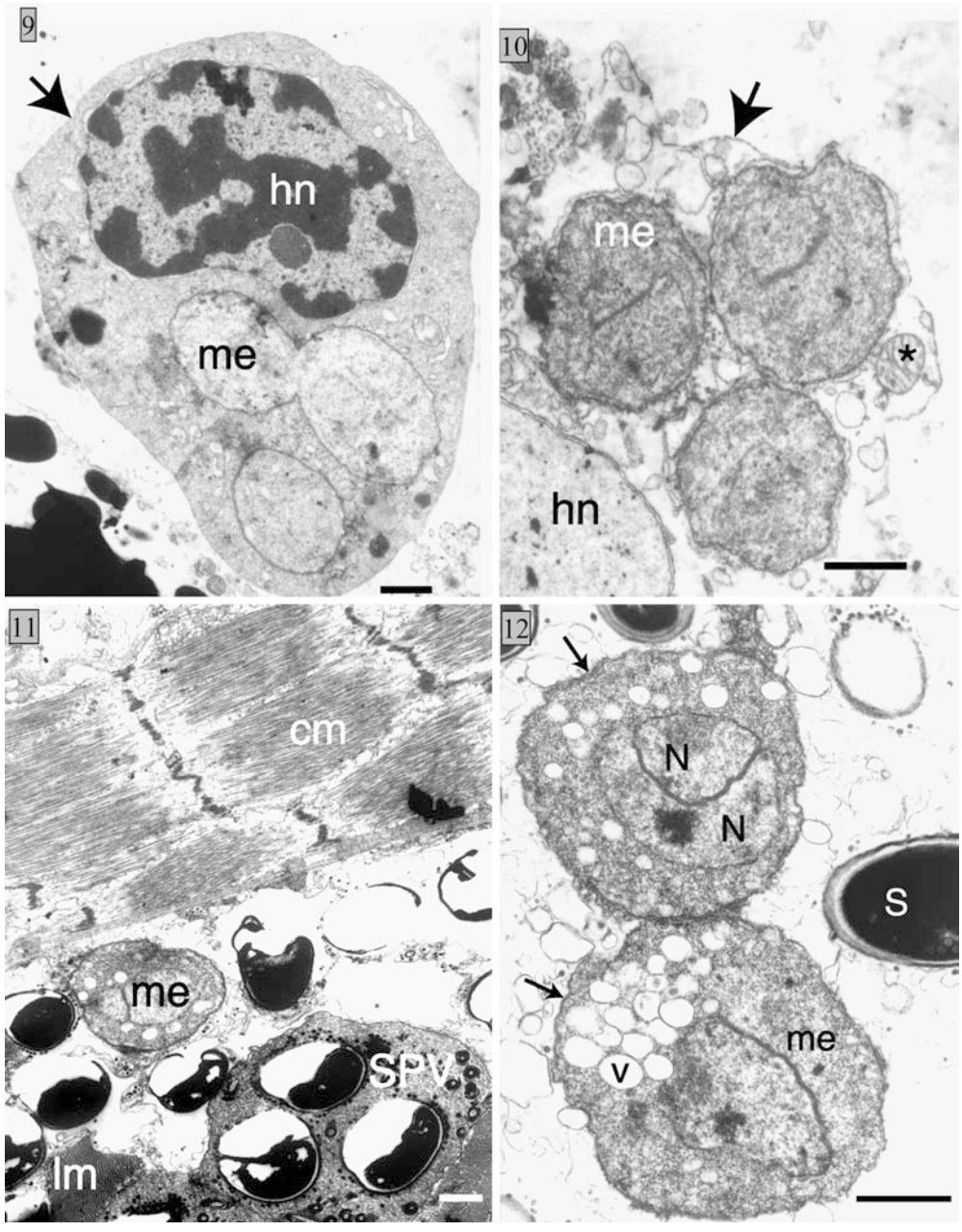

Fig. 9 Dividing meront (*me*) inside a haemocyte (→) in crayfish hepatopancreas; haemocyte nucleus (*hn*). *Scale bar* 1 μm

Fig. 10 Three late-stage meronts inside haemocyte (→) in crayfish hepatopancreas; haemocyte nucleus (*hn*), mitochondrion (*). *Scale bar* 1 μm

Fig. 11 Late meront/early sporont (*me*) in intestinal wall between circular muscle layer (*cm*) and bundles of longitudinal muscle fibres (*lm*). SPVs containing mature spores also visible. *Scale bar* 1 μm

Fig. 12 Late meront/early sporont stages (*me*) with numerous vesicles (*v*), diplokaryotic nuclei (*N*) and electron-dense deposits on plasmalemma (→). Mature spore (*S*) in same host muscle cell. *Scale bar* 1 μm

Sporoblasts

Binucleate sporonts within SPVs (Fig. 13) divided to form multinucleate plasmodia in the form of a rosette (Figs. 18, 19, 20), from which eight uninucleate sporoblasts were pinched off (Figs. 21, 22). Prominent nucleoli were often seen in sections of more mature sporoblasts. A dense circular body was evident at the base of each sporoblast in the region where the cell would later separate from the rosette (Fig. 20). The circular bodies were very similar to those illustrated in electron micrographs of *T. duorara* sporoblasts (Iversen et al. 1987).

Development of the spore coat of uninucleate spores was associated with high densities of microtubules in the episporontal space of the SPV (Fig. 21). Relatively low densities of microtubules were seen in the vicinity of developing binucleate spores (Fig. 23). The spore coat of binucleate spores was laid down in interrupted sections (Fig. 24). Structures similar to spindle plaques were seen in the nuclei of binucleate sporoblasts (Fig. 25).

Mature uninucleate spores remained in persistent SPVs, whereas mature binucleate spores were generally found in direct contact with host cytoplasm. No evidence was found for SPV formation around sporonts (Fig. 14) or spores (Fig. 26) within haemocytes.

Mature spores

Free binucleate spores and uninucleate spores within SPVs occurred in the same myocytes. The isofilar polar

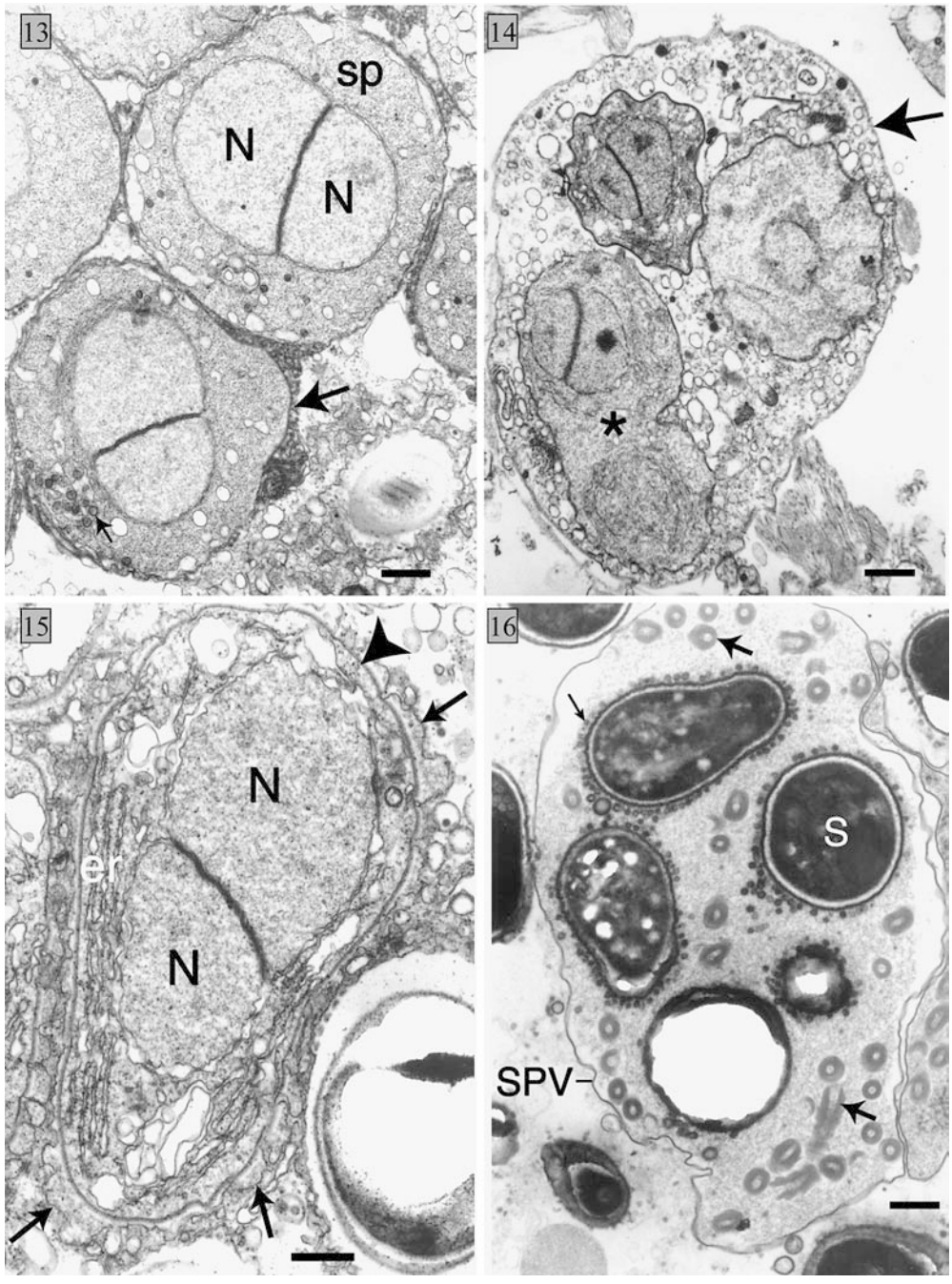

Fig. 13 Sporonts (*sp*) in yabby myocyte. Nuclei (*N*) are diplokaryotic. Early formation of SPV (*large arrow*) around sporonts evident. Mitochondrial remnant-like structures (*small arrow*) visible. *Scale bar* 1 μm

Fig. 14 Three sporonts at different stages of maturation within a haemocyte (→). One of the sporonts (*) is dividing. *Scale bar* 1 μm

Fig. 15 An elongated sporont in crayfish myocyte with envelope (→) developing adjacent to thickened plasmalemma (→). Nuclei (*N*) are diplokaryotic and endoplasmic reticulum (*er*) well developed. *Scale bar* 1 μm

Fig. 16 SPV with macrotubules (*large arrows*) and microtubules (*small arrow*) around spores (*s*) in episporontal space. *Scale bar* 500 nm

filament of binucleate spores was coiled 6–8 times at the anterior end of the posterior vacuole (Figs. 27, 28, 29, 30), whereas 12–20 coils of the isofilar polar filament could be seen in cross-section in uninucleate spores (Figs. 31, 32). The average diameter of the polar filament in binucleate spores was 83 nm (range 65–102 nm, $n = 42$), compared to 59 nm (53–74 nm, $n = 32$) in uninucleate spores.

The ultrastructural features of binucleate spores are illustrated in Fig. 30. The nuclei were always closely apposed to form a diplokaryon. The polaroplast was lamellar in nature, with dense parallel arrays of membranes that readily took up stain in the anterior polaroplast, giving it the appearance of a dark crescent within the spore. The lamellae in the posterior polaroplast were more widely spaced. The posterior vacuole appeared as either a collection of vesicles or an empty space, surrounded by the coils of the polar filament. Numerous ribosomes were scattered through the cytoplasm.

The exospore layer of binucleate spores was 30–40 nm wide, when measured adjacent to the coils of the polar filament, whereas the endospore layer was more than twice as thick (Fig. 28). The average exospore and endospore layer widths of uninucleate spores (Figs. 31, 32) were 24 nm (20–40 nm, $n = 9$), and 73 nm (56–110 nm, $n = 9$), respectively. Exospore and endospore layers were

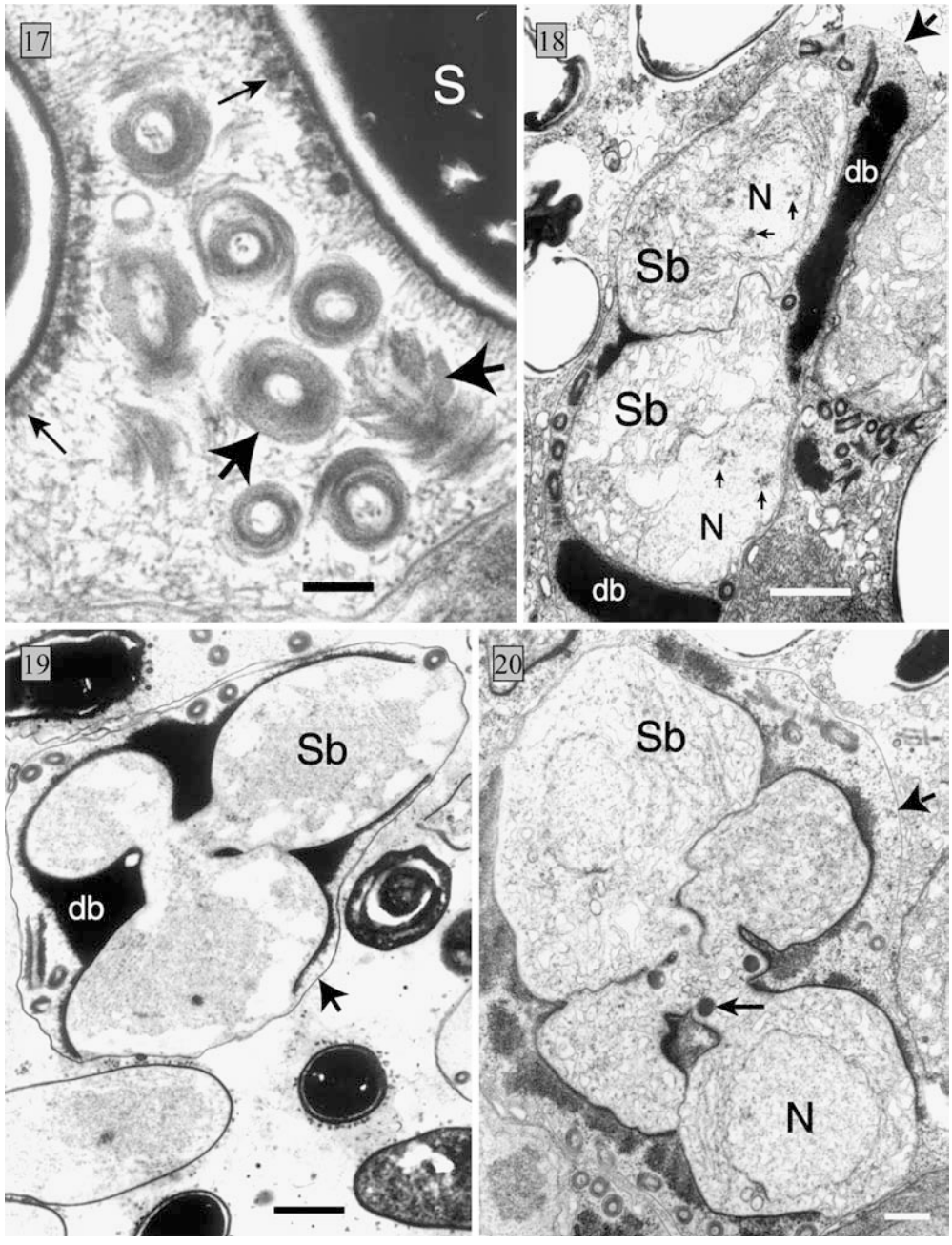

Fig. 17 Microtubules (*small arrows*) adjacent to mature spores (*S*) and macrotubules (*large arrows*) composed of stacked coils of fibres. *Scale bar* 200 nm

Fig. 18 Dense bodies (*db*) closely associated with developing sporoblasts within a SPV (*large arrow*). Sporoblasts are uninucleate at this stage, with two regions of concentrated chromatin (*small arrows*) visible in each nucleus (*N*). *Scale bar* 1 μm

Fig. 19 Rosette of incompletely divided sporoblasts (*Sb*) in SPV (→) in close association with large dense body (*db*). *Scale bar* 1 μm

Fig. 20 Rosette of incompletely divided sporoblasts (*Sb*) in SPV (*large arrow*), each with an electron-dense circular body (*small arrow*) near the centre of the rosette. Single nucleus (*N*) in each sporoblast. *Scale bar* 1 μm

usually narrower over the polar capsule. Shrinkage of the spore cytoplasm and plasmalemma away from the spore coat in fixed specimens frequently occurred.

In the crayfish from Tumut with a very heavy infection of *T. parastaci* sp. nov., many of the spores appeared to have degenerated (Fig. 33) and haemocytes containing degraded spore material were relatively common (Fig. 34).

Ribosomal DNA sequence analysis

SSU rDNA sequences were determined for samples indicated in Table 1. Sequences from samples WW1, WA1, R1 and R7 were submitted to Genbank with accession nos. AF294781, AF294780, AF294779 and AF534878, respectively. The partial ITS sequence of sample R1 and the entire ITS sequences of samples WA1 and R7 were included in the submissions. The first 40 bp of the SSU rDNA gene of *T. parastaci* sp. nov., downstream from the 5′ end of the 18f primer, were not included in the Genbank submissions as this portion was only sequenced in one direction.

T. parastaci sp. nov. and *T. contejeani* showed 92% sequence identity across 1,299 bp of SSU rDNA sequence. No close relationship with any other described species on the Genbank database was indicated. *T. parastaci* sp. nov. showed 67% sequence identity with

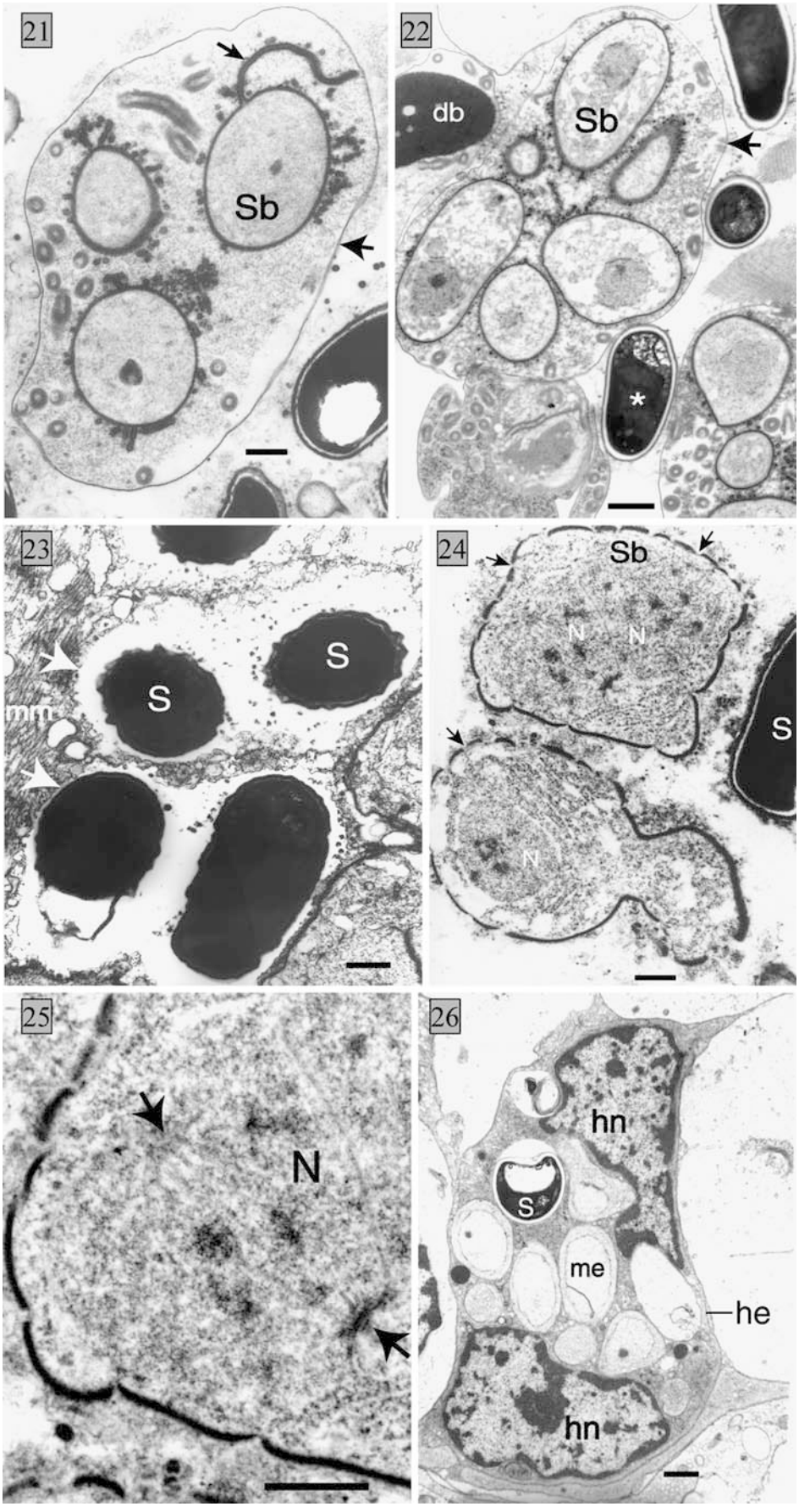

Fig. 21 Microtubules apparently involved with formation of the spore coat (*small arrow*) of an immature sporoblast within an SPV (*large arrow*). *Scale bar* 500 nm

Fig. 22 Separate sporoblasts (*Sb*) within SPV (→), adjacent to dense body (db) of less mature SPV, and a free diplokaryotic spore (*). *Scale bar* 1 μm

Fig. 23 Delicate vesicles (→) in direct contact with muscle fibres (*mm*), surrounding pairs of diplokaryotic spores (*S*). *Scale bar* 500 nm

Fig. 24 Interrupted sections (→) of electron dense material deposited on the plasmalemma of binucleate sporoblasts (*Sb*) adjacent to a mature free spore (*S*) in a crayfish myocyte. *Scale bar* 1 μm

Fig. 25 Enlarged left nucleus (*N*) from binucleate sporont in Fig. 24. Spindle plaques visible (→). *Scale bar* 1 μm

Fig. 26 Meronts (*me*) and a mature spore (*S*) within a haemocyte (*he*) in crayfish hepatopancreas. Two lobes of haemocyte nucleus (*hn*) are visible. *Scale bar* 1 μm

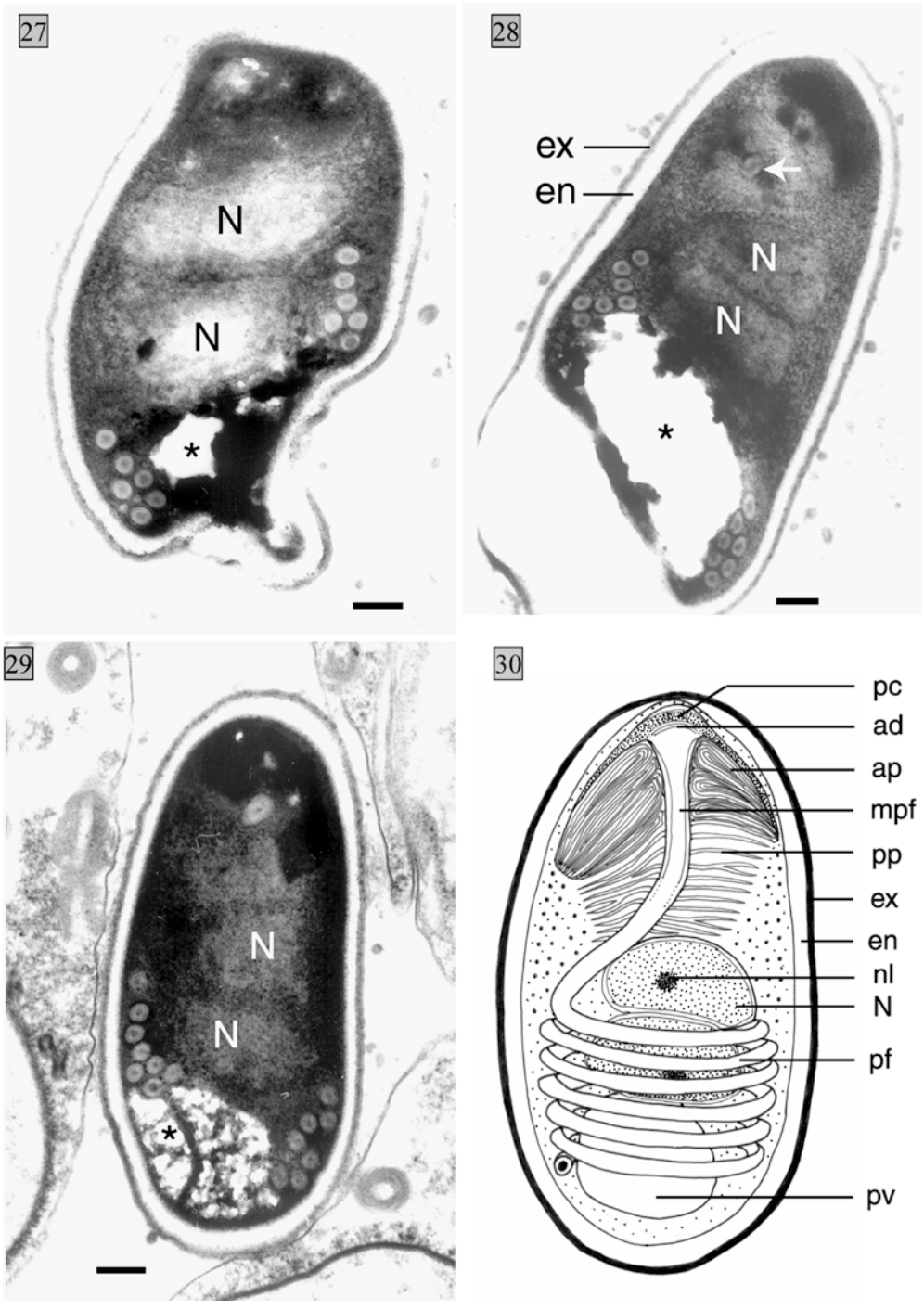

Fig. 27 Binucleate free spore with diplokaryotic nuclei (*N*). Six coils of the polar filament can be seen in transverse section lateral to the posterior vacuole (*). *Scale bar* 200 nm

Fig. 28 Diplokaryotic spore with seven coils of the polar filament in transverse section, lateral to the posterior vacuole (*). A portion of the manubrium of the polar filament (→) can be seen anterior to the nuclei (*N*). The endospore layer (*en*) is more than twice as thick as the exospore layer (*ex*) of the spore coat. *Scale bar* 200 nm

Fig. 29 A free binucleate spore with eight coils of the polar filament latero-caudal to the second of the two nuclei (*N*). The posterior vacuole (*) appears divided by cytoplasmic remnants. *Scale bar* 200 nm

Fig. 30 Diagram of ultrastructural features of binucleate spore. Polar capsule (*pc*), anchoring disc (*ad*), anterior polaroplast (*ap*), manubrium of polar filament (*mpf*), posterior polaroplast (*pp*), exospore layer of spore coat (*ex*), endospore layer of spore coat (*en*), nucleolus (*nl*), nucleus (*N*), polar filament (*pf*), posterior vacuole (*pv*)

the fire ant pathogen *T. solenopsae* (Genbank accession no. AF031538.1). GC content in the SSU rDNA of *T. parastaci* sp. nov. was 40%. The gene, including the primers 18f and 1492r, was 1,337 bp long in *T. parastaci* sp. nov. and 1,361 bp long in *T. contejeani*. The SSU and ITS rDNA sequences of *T. parastaci* sp. nov. from West Wimmera (Victoria), Western Australia and Tumut (southern New South Wales) were identical, indicating that the same microsporidian species was infecting these *C. d. albidus* yabbies. In *T. parastaci* sp. nov. from *C. d. rotundus* yabbies (Karuah system), four single nucleotide sites in the SSU rDNA and one site in the ITS region, were ambiguous. The ambiguous sites were located 60 (A/G), 694 (A/T), 716 (A/G), 1,125 (A/G) and 1,403 (A/T) bp downstream from the 5′ end of the 18f primer. The nature of each ambiguity is indicated in parentheses. One of the two possible nucleotides at each of the ambiguous sites in *T. parastaci* sp. nov. from "*rotundus*" yabbies was present, but not ambiguous in the sequences of *T. parastaci* sp. nov. from "*albidus*" yabbies. The differences may have been due to sequencing anomalies or polymorphisms at these sites in the *C. d. rotundus*

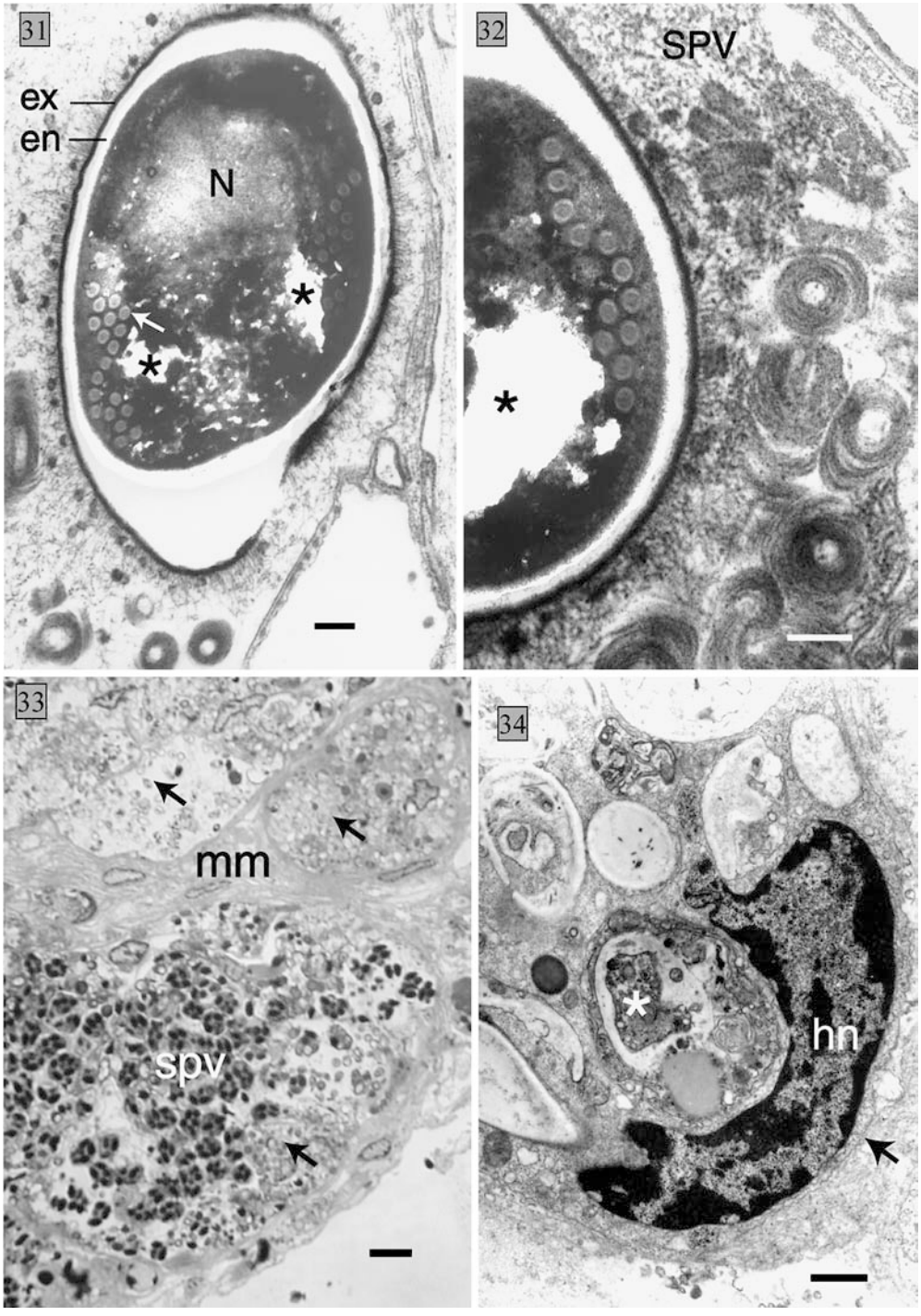

Fig. 31 Uninucleate (*N*) spore within SPV. Twenty coils of the polar filament () can be seen in transverse section, adjacent to the posterior vacuole (*). The endospore (*en*) is more than twice as thick as the exospore layer. *Scale bar* 200 nm

Fig. 32 Spore within SPV showing 12 coils of the polar filament in transverse section, lateral to the posterior vacuole (*). *Scale bar* 200 nm

Fig. 33 Light micrograph of a toluidine-stained section of heavily infected crayfish muscle. Areas of degenerating spores (→) are visible adjacent to normal mature spores within SPVs. Normal muscle cell architecture (*mm*) has been disrupted in infected cells. Scale bar 10 μm

Fig. 34 Electron micrograph of degenerating spore material (*) adjacent to haemocyte nucleus (*hn*) within a haemocyte (→), in crayfish muscle tissue. *Scale bar* 1 μm

population sampled. They did not provide sufficient grounds to relegate the microsporidians from *C. d. rotundus* to a different species. The similarities in ultrastructure between the *C. d. albidus* and *C. d. rotundus* samples support this view.

Discussion

Similarities in morphological features, including ultrastructure of spores and SPVs, and similarities in SSU rDNA sequences, indicate that *T. parastaci* sp. nov. is congeneric with *T. contejeani,* as described by Cossins and Bowler (1974), Vivares (1975) and Lom et al. (2001). The species descriptor "*parastaci*" indicates that members of the Australian freshwater crayfish family Parastacidae serve as hosts for this parasite. Lom et al. (2001) raised the issue of whether *T. contejeani* should remain in the genus *Thelohania*, in view of the absence of diplokaryotic spore stages in other microsporidian species in the genus, including *T. maenadis* Perez, 1904, and *T. octospora* Henneguy, 1892, which are parasites

of marine decapods. The same concerns apply to *T. parastaci* sp. nov. The issue is unlikely to be resolved until molecular data from other *Thelohania* species, in particular the type species *T. giardi*, are available for comparison. SSU rDNA sequence data from this study and others (Lom et al. 2001; Moodie et al. 2003) indicate that *T. parastaci* sp. nov. and *T. contejeani* are more closely related to the *Vairimorpha/Nosema* group of species than to the fire ant pathogen *T. solenopsae* (Moser et al. 1998), i.e. the crayfish and fire ant parasites are not congeneric.

The family to which *T. parastaci* sp. nov. should be assigned is also problematic in view of uncertainties with respect to traditional taxonomy of the Microspora, in the light of new molecular and morphological data that have recently become available (Weiss and Vossbrinck 1998; Larsson 1999). In the most recent review of microsporidian classification, Sprague et al. (1992) assigned *Thelohania* to the family Thelohaniidae Hazard & Oldacre, 1975; superfamily Thelohanioidea Hazard & Oldacre, 1975; order Meiodihaplophasida ord. n; Class Dihaplophasea cl. n. Members of the superfamily Thelohanioidea were defined as having spores of only one morphological type. As *T. parastaci* is at least dimorphic, this definition would disqualify it from the superfamily Thelohanioidea and the family Thelohaniidae. Lom et al. (2001) comment that *T. contejeani* and *T. solenopsae* have life cycles similar in nature to members of the family Burenellidae Jouvenaz and Hazard 1978, which includes genera with both a octoblastic sporulation sequence producing uninucleate spores in a SPV, and a binucleate sporulation sequence producing free spores. Phylogenetic studies based on a more extensive array of molecular and morphological data than are currently available will hopefully resolve these uncertainties in the future.

The full host range of *T. parastaci* sp. nov. was not investigated, and it is possible that an intermediate host may be infected by the uninucleate spores, such as occurs in the genera *Amblyospora* Hazard and Oldacre, 1975 (Becnel and Andreadis 1999) and *Hyalinocysta* Hazard and Oldacre, 1975 (Andreadis and Vossbrinck 2002). Species other than *C. destructor* may also serve as hosts for *T. parastaci* sp. nov. Langdon and Thorne (1992) were able to experimentally transmit *Vavraia parastacida* Langdon 1991, a microsporidian parasite of marron (*C. tenuimanus*), to yabbies (*C. destructor*), although natural infections were not detected in the latter.

A hypothetical life cycle for *T. parastaci* sp. nov. is illustrated in Fig. 35. The stage of octoblastic sporogony at which meiosis occurred in *T. parastaci* sp. nov. was not observed; however, in view of other similarities to *T. contejeani*, meiosis is likely to be initiated in the sporont, as described by Lom et al. (2001). The quadrinucleate SPVs are presumably the result of meiosis II, with a final mitotic division resulting in octosporous vesicles with uninucleate (haploid) spores (Flegel and Pasharawipas 1995). The frequent occurrence of pairs of diplokaryotic spores in Giemsa-stained impression smears of muscle and other tissues, the spindle plaques in Fig. 25 and the nature of the vesicles around the binucleate spores in Fig. 23 suggest they are produced by binary fission of the sporont, as described by Lom et al. (2001) for *T. contejeani*.

Infection of haemocytes by *T. parastaci* indicates these cells may play a role in distributing infective spores to other tissues in the body, as has been shown for other microsporidians (David and Weiser 1994), and lends weight to the as yet unproven hypothesis that infective stages may enter the host via the digestive tract (Voronin 1971), to be taken up by haemocytes and transported in these cells to other tissues such as muscle, where further multiplication produces massive numbers of spores for transmission to the next host. Merogony of *T. maenadis*, a crab parasite, was reported to occur in both haemolymph and muscle tissue; however, meronts in the haemolymph were described as uninucleate (Canning and Vavra 2000).

Vertical transmission has not been confirmed for any *Thelohania* species parasitising a crustacean host, although *T. contejeani* has been reported to infect eggs, ovarian tissue and the enveloping tissues around the ovary of *Astacus* crayfish (Voronin 1971; Vey and Vago 1973; Cossins and Bowler 1974). No spores or earlier stages of *T. parastaci* sp. nov. were found in ovarian tissue. However, only a few specimens were examined and vertical transmission of the parasite cannot be ruled out. In situ hybridization, a means of visually tagging small fragments of DNA unique to the parasite (Carville et al. 1997), may offer a more effective means for studying tissue tropism of *T. parastaci* sp. nov. than conventional histological methods.

It is somewhat surprising that the rDNA sequences of samples of *T. parastaci* sp. nov. were almost identical between samples from *C. d. rotundus* yabbies in the Karuah River system in New South Wales and *C. d. albidus* yabbies in the West Wimmera region, thousands of kilometres south on a different river system. *C. d. rotundus* and *C. d. albidus* populations have been separated long enough for their rDNA to become genetically distinct (Austin 1996; Crandall et al. 1999), so why are there not more substantial genetic differences in the rDNA of their parasites? It is possible that some degree of mixing of the *T. parastaci* sp. nov. populations still occurs due to the transport of spores between regions, in the digestive tracts of migratory water birds that feed on yabbies. Movement of infected yabbies by yabby farmers between regions may have the same effect. The Western Australian yabbies from which samples were taken were probably originally sourced from the West Wimmera region, therefore one would expect *T. parastaci* sp. nov. from these two regions to be identical. Sequencing of multiple clones would be necessary to confirm that the five sites of ambiguous nucleotide identity in the rDNA of *T. parastaci* sp. nov. from *C. d. rotundus* were genuine polymorphisms, rather than sequencing anomalies.

Early developmental stages and spores of *T. parastaci* sp. nov. within intact myocytes and haemocytes

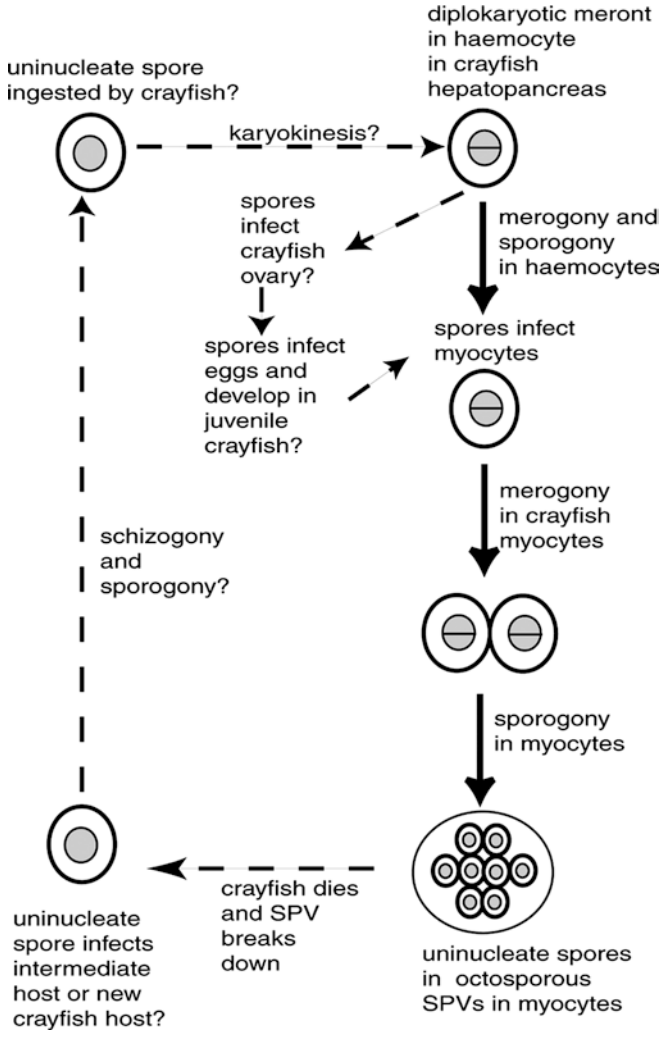

Fig. 35 A hypothetical life cycle for *T. parastaci*

are apparently protected from a cellular immune response by the host. Tissue haemocytes were seen in the vicinity of spores and phagocytosing spore material in only one very heavily infected specimen. Studies of microsporidian parasites of vertebrate hosts indicate that clinical signs of infection are usually, but not always, associated with a decline in immune competence of the host, and that chronic latent infections in healthy hosts can be reactivated if immunosuppression occurs (Didier 2000). The same may hold true for crayfish. Death as a result of infection by *T. parastaci* should not be considered inevitable until transmission experiments, which track the progress of infection under different physiological conditions, have been carried out. The yabby host of *T. parastaci* sp. nov. lives in streams and water bodies subject to dramatic fluctuations in water quality. These fluctuations may act as physiological stressors that reduce immune competence and increase host susceptibility to infection (France and Graham 1985).

Cherax destructor is an economically important species in Australia, with production in aquaculture systems forecast to increase substantially over the next few years (Piper 2000; Ruello 2002). Thelohaniasis is a potentially significant disease of both cultured and wild stocks. It is hoped that the data presented in this study will provide tools with which to further investigate the biogeography, epizootology and transmission pathways of *T. parastaci* sp. nov. and related species. As a result of such studies, the ecological roles of microsporidian parasites in wild populations of crayfish could be elucidated, and strategies for effective prevention and control of thelohaniasis in cultured populations developed.

Taxonomic summary—*Thelohania parastaci* sp. nov.

Type host The freshwater crayfish *Cherax destructor albidus* (Austin 1996), *C. d. rotundus* (Austin 1996), *C. d. destructor* (Austin 1996).

Transmission Unknown.

Site of infection Muscle tissue.

Host-parasite interface Uninucleate spores produced in sporophorous vesicles of parasite origin. Meronts, early sporonts and diplokaryotic spores in direct contact with host cell cytoplasm.

Merogony Diplokaryotic meronts found in muscle tissue, intestinal wall, haemocytes. Meronts in haemocytes spindle shaped. Meronts in other tissues round in shape.

Transition to sporogony Sporonts diplokaryotic, round in shape and identified by thickening of parasite plasmalemma with highly vacuolated / vesicular cytoplasm.

Sporogony Simultaneous dimorphic sporogony in muscle tissue. One sporogony pathway involves binary fission with production of diplokaryotic spores in contact with host cell cytoplasm. The other sporogony pathway involves formation of a sporophorous vesicle with production of up to eight uninucleate spores per vesicle, presumably by meiosis. Sporogony in haemocytes involves binary fission. SPVs not observed in haemocytes.

Binucleate spores Diplokaryotic. Lozenge shaped. Average fresh spore length: 3.9 (3.2–4.9) μm. Average fresh spore width: 2.0 (1.5–2.7) μm. Isofilar polar filament with 6–8 coils, 83 (65–102) nm in diameter. Lamellar polaroplast. Lateral exospore width: 34 (30–40) nm. Lateral endospore width: 58 (50–60) nm.

Uninucleate spores Develop from a rosette shaped plasmodium inside sporophorous vesicle. Lozenge shaped. Isofilar polar filament with 12–20 coils, 59 (53–74) nm in diameter. Lateral exospore width: 24 (20–40) nm. Lateral endospore width: 73 (56–110) nm.

Sporophorous vesicles Of parasite origin. Average vesicle diameter 8.8 (7.4–10.5) μm. 8 spores per vesicle. Contain macrotubules: 249 (205–307) nm in diameter, microtubules: 73 (50–99) nm in diameter, and early in sporoblast development, granular dense bodies.

Type locality Hapantotype: West Wimmera region, Victoria, Australia. (37° 4′ S, 141° 19′ E)

Type specimens Giemsa stained smears were submitted to the Queensland Museum, Brisbane, Australia. Hapantotype submission number: G463715. Parahapantotype submission numbers: G463716, G463717, G463718, G463719.

Molecular data 16S SSU rDNA sequenced directly, Genbank accession numbers: Hapantotype: AF294781, Parahapantotypes: AF294780, AF294779, AF534878. ITS rDNA directly sequenced and included in Genbank accessions: AF294780, AF294779, AF534878.

Remarks *Cherax destructor*, the host of *T. parastaci* sp. nov., belongs to the Australian freshwater crayfish family Parastacidae. The descriptor *parastaci* is derived from Latin and refers to the family of the host species.

Acknowledgements This research was supported by a joint scholarship from the University of New England and CSIRO, Livestock Industries. The authors particularly wish to thank the following people for their assistance: Dr. Robert Adlard, Mr. Justin Bellanger, Dr. Carlos Azevedo, Mr. Trevor Domachenz, Mrs. Maxine Domachenz, Prof. Iva Dykova, Mr. Zoltan Enoch, Mr. Peter Garlick, Prof. Robin Gasser, Mr. Paul Hillier, Dr. Dean Jerry, Dr. Brian Jones, Ms. Mahri Koch, Dr. Jennifer Mathews, Ms. Clare Meyer, Dr. Mary Notestine, Dr. Peter O'Donoghue, Dr. Tony Sweeney, Prof. Klaus Rohde, Mr. Callum Mack and Mr. Ian Lenane.

References

Alderman DJ, Polglase JL (1988) Pathogens, parasites and commensals. In: Holdich DM, Lowery RS (eds) Freshwater crayfish: biology, management and exploitation. Croom Helm, London, pp 167–212

Altschul SF, et al. (1997) Gapped BLAST and PSI-BLAST: a new generation of protein database search programs. Nucleic Acids Res 25:3389–3402

Andreadis TG, Vossbrinck CR (2002) Life cycle, ultrastructure and molecular phylogeny of *Hyalinocysta chapmani* (Microsporidia: Thelohaniidae), a parasite of *Culiseta melanura* (Diptera: Culicidae) and *Orthocyclops modestus* (Copepoda: Cyclopidae). J Eukaryot Microbiol 49:350–364

Austin CM (1996) Systematics of the freshwater crayfish genus *Cherax* Erichson (Decapoda: Parastacidae) in northern and eastern Australia: electrophoretic and morphological variation. Aust J Zool 44:259–296

Becnel JJ, Andreadis TG (1999) Microsporidia in insects. In: Wittner M, Weiss LM (eds) The Microsporidia and microsporidiosis. ASM Press, Washington, D.C., pp 447–501

Canning EU, Vavra J (2000) Phylum Microsporida. In: Lee JJ, Leedale GF (eds) An illustrated guide to the Protozoa, second edition. Society of Protozoologists, Kansas, pp 39–126

Carstairs IL (1979) Report of microsporidial infestation of the freshwater crayfish, *Cherax destructor*. Freshw Crayfish 4:343–347

Carville A, Mansfield K, Widmer G, Lackner A, Kotler D, Weist P, Gumbo T, Sarbah S, Tzipori S (1997) Development and application of genetic probes for detection of *Enterocytozoon bieneusi* in formalin-fixed stools and in intestinal biopsy specimens from infected patients. Clin Diagn Lab Immunol 4:405–408

Cossins AR (1973) *Thelohania contejeani* Henneguy. Microsporidian parasite of *Austropotamobius pallipes* Lereboullet—an histological and ultrastructural study. Freshw Crayfish 1:151–164

Cossins AR, Bowler K (1974) An histological and ultrastructural study of *Thelohania contajeani* Henneguy, 1892 (Nosematidae), microsporidian parasite of *Austropotamobius pallipes* Lereboullet. Parasitology 68:81–91

Crandall KA, Fetzner JWJ, Lawler SH, Kinnersley M, Austin CM (1999) Phylogenetic relationships among the Australian and New Zealand genera of freshwater crayfishes (Decapoda: Parastacidae). Aust J Zool 47:199–214

David L, Weiser J (1994) Role of hemocytes in the propagation of a microsporidian infection in larvae of *Galleria mellonella*. J Invertebr Pathol 63:212–213

Didier ES (2000) Immunology of microsporidiosis. In: Petry F (ed) Cryptosporidiosis and microsporidiosis. Karger, Basel, pp 193–208

Flegel TW, Pasharawipas T (1995) A proposal for typical eukaryotic meiosis in microsporidians. Can J Microbiol 41:1–11

France RL, Graham L (1985) Increased microsporidian parasitism of the crayfish *Orconectes virilis* in an experimentally acidified lake. Water Air Soil Pollut 25:129–136

Henneguy G, Thelohan P (1892) Myxosporides parasites des muscles chez quelques crustaces decapodes. Ann Microgr 4:617–641

Iversen ES, Kelly JF, Alzamora D (1987) Ultrastructure of *Thelohania duorara* Iversen & Manning, 1959 (Microspora, Thelohaniidae) in the pink shrimp, *Penaeus duorarum* Burkenroad. J Fish Dis 10:299–307

Jones JB, Lawrence CS (2001) Diseases of yabbies (*Cherax albidus*) in Western Australia. Aquaculture 194:221–232

Knell JD, Allen GE, Hazard EI (1977) Light and electron microscope study of *Thelohania solenopsae* n. sp. (Microsporida: Protozoa) in the red imported fire ant, *Solenopsis invicta*. J Invertebr Pathol 29:192–200

Langdon JS (1991) Microsporidiosis due to a pleistophorid in marron, *Cherax tenuimanus* (Smith), (Decapoda: Parastacidae). J Fish Dis 14:33–44

Langdon JS, Thorne T (1992) Experimental transmission per os of microsporidiosis due to *Vavraia parastacida* in the marron, *Cherax tenuimanus* (Smith) and yabby, *Cherax albidus* (Clark). J Fish Dis 15:315–322

Larsson JIR (1999) Identification of microsporidia. A review. Acta Protozool 38:161–197

Lom J, Nilsen F, Dykova I (2001) *Thelohania contejeani* Henneguy, 1892: dimorphic life cycle and taxonomic affinities, as indicated by ultrastructural and molecular study. Parasitol Res 87:860–872

Moodie EG, Le Jambre LF, Katz ME (2003) *Thelohania montirivulorum* sp. nov. (Microspora: Thelohaniidae), a parasite of the Australian freshwater crayfish, *Cherax destructor* (Decapoda: Parastacidae): fine ultrastructure, molecular characteristics and phylogenetic relationships. Parasitol Res (in press)

Moser BA, Becnel JJ, Maruniak J, Patterson RS (1998) Analysis of the ribosomal DNA sequences of microsporidia *Thelohania* and *Vairimorpha* of Fire Ants. J Invertebr Pathol 72:154–159

O'Donoghue PJ, Adlard RD (2000) Catalogue of Protozoan parasites recorded in Australia. In: Memoirs of the Queensland Museum. Queensland Museum, Brisbane, Australia, 45:1–163

O'Donoghue P, Beveridge I, Phillips P (1990) Parasites and ectocommensals of yabbies and marron in South Australia. Central Veterinary Laboratories (VETLAB), South Australian Department of Agriculture, Adelaide, South Australia

Piper L (2000) Potential for expansion of the freshwater crayfish industry in Australia: a report for the Rural Industries Research and Development Corporation. Rural Industries Research and Development Corporation, Canberra, p 32

Quilter CG (1976) Microsporidian parasite *Thelohania contejeani* Henneguy from New Zealand freshwater crayfish. NZ J Mar Freshw Res 10:225–231

Rhoads DD, Roufa DJ (1990) SEQAIDII, a comprehensive PC software package for analysis of nucleic acid and protein sequence data. Available in the public domain on international molecular biological software servers. 3.8 edn. University of Kansas, Kansas

Ruello NV (2002) Report on yabby marketing cooperative feasibility study prepared for NSW Fisheries and the Department of State and Regional Development. Ruello and Associates, Sydney, NSW

Sindermann CJ (1990) Principal diseases of marine fish and shellfish. Academic Press, San Diego, Calif.

Sprague V (1950) *Thelohania cambari* n. sp., a microsporidian parasite of North American crayfish. J Parasitol Suppl 36:46

Sprague V, Becnel JJ, Hazard EJ (1992) Taxonomy of phylum Microspora. Crit Rev Microbiol 18:285–395

Swofford DL (2000) PAUP*. Phylogenetic analysis using parsimony (*and other methods), version 4. Sinauer, Sunderland, Mass.

Undeen A (1997) Microsporidia (Protozoa): A Handbook of Biology and Research Techniques. http://www.okstate.edu/OSU_Ag/agedcm4h/ag_news/SCSB387.htm. Center for Medical, Agricultural and Veterinary Entomology, Gainesville, Florida, USA

Vey A, Vago C (1973) Protozoan and fungal diseases of *Austropotamobius pallipes* Lereboullet in France. Freshw Crayfish

Vivares CP (1975) Etude comparative faite en microscopies photonique et electronique de trois especes de microsporidies appartenant au genre *Thelohania* Henneguy, 1892, parasites de crustaces decapodes marins. Ann Sci Nat Zool 17:141–178

Voronin VN (1971) New data on microsporidiosis of the crayfish *Astacus astacus* (L. 1758). Parazitologiya 5:186–191

Weiss LM, Vossbrinck CR (1998) Microsporidiosis: molecular and diagnostic aspects. In: Tzipori S (ed) Opportunistic Protozoa in humans. Academic Press, London, pp 351–395

Williams BAP, Hirt RP, Lucocq JM, Embley TM (2002) A mitochondrial remnant in the microsporidian *Trachipleistophora hominis*. Nature 418:865–869